Human plasma retinol-binding protein (RBP4) is also a fatty acid-binding protein

Massimiliano Perduca*, Stefania Nicolis[#], Barbara Mannucci[§], Monica Galliano[‡] and Hugo L. Monaco*

From the [*]Biocrystallography Laboratory, Department of Biotechnology, University of Verona, Ca Vignal 1, strada Le Grazie 15, 37134 Verona, Italy, [#]Department of Chemistry, via Torquato Taramelli 12, [§]Centro Grandi Strumenti (CGS), via Agostino Bassi 21 and [‡]Department of Molecular Medicine via Taramelli 3b, University of Pavia, 27100 Pavia, Italy.

* Correspondence e-mail: hugo.monaco@univr.it

Running title: Human RBP4 not bound to retinol has a fatty acid molecule in its ligand biding site.

Synopsis

RBP4, plasma retinol-binding protein, is the specific transporter of the vitamin in the plasma of vertebrates. This paper reports that the transporter isolated from sources in which the molecules are expected to be in their apo form have a fatty acid molecule bound in the central cavity of the protein.

Keywords: RBP4, plasma retinol-binding protein; X-ray structure; lipocalin, TTR, transthyretin, formerly called prealbumin; fatty acid.

Abstract

RBP4 (plasma retinol-binding protein) is the 21 kDa transporter of all-trans retinol that circulates in plasma as a moderately tight 1:1 molar complex of the vitamin with the protein. RBP4 is primarily synthesised in the liver but is also produced by adipose tissue and circulates bound to a larger protein, transthyretin, TTR, that serves to increase its molecular mass and thus avoid its elimination by glomerular filtration.

This paper reports the high resolution three-dimensional structures of human RBP4 naturally lacking bound retinol purified from plasma, urine and amniotic fluid. In all these crystals we found a fatty acid molecule bound in the hydrophobic ligand-binding site, a result confirmed by mass spectrometry measurements.

In addition we also report the 1.5 Å resolution structures of human holo-RBP4 and of the protein saturated with palmitic and lauric acid and discuss the interaction of the fatty acids and retinol with the protein.

Introduction

The specific transport system for vitamin A in the plasma of vertebrates consists of a 21 kDa protein with a single binding site for retinol called retinol-binding protein 4 (RBP4)[1], structurally the prototype of the well-known hydrophobic ligand binding protein family of the lipocalins[2]. RBP4 is primarily synthesised in the liver but it is also produced by adipose tissue (about 20-40 % of the amounts released by the liver). The holo form of RBP4 with one molecule of all-trans retinol in its ligand-binding site associates with a higher molecular weight plasma protein called transthyretin (TTR, formerly called prealbumin[3,4]), a 55 kDa homo-tetramer involved in the transport of thyroid hormones[5]. When the molecular complex RBP-TTR encounters the RBP receptor, STRA6[6], holo-RBP dissociates from the complex to bind to STRA6 which transports the vitamin into the cell. The remaining RBP4 depleted from retinol has a substantially lower affinity for TTR and travels in plasma mostly dissociated and, since its molecular weight is relatively low, it is removed from circulation by filtration in the kidneys[7]. Its final fate is urine (or amniotic fluid in the case of the developing foetus), a source from which the protein unbound to retinol can be purified, and in high yields, if the sample is obtained from patients with glomerulotubular proteinuria[8,9].

The X-ray structures of all the players in this mechanism are well known, in particular those of human holo[10] and presumed apo-RBP[11] were published at 2.0 and 2.5 Å respectively for the proteins purified from plasma and to 1.7 Å for the recombinant protein unbound to retinol[12]. The structure of STRA6, the receptor of holo RBP4 was also determined more recently[13]. The question of what happens to RBP4 when the retinol molecule is removed from its binding cavity has received attention for a long time. The initial suggestion of a total collapse of the molecular architecture[14] was put in doubt following the publication of the structures of RBP4 not bound to retinol describing minimal conformational changes that are consistent with the interactions RBP-TTR observed in the X-ray structure of the RBP-TTR complex[15,16]. In the central cavities of all the molecules that did not contain retinol, residual electron density was always observed that was interpreted as solvent molecules in the 2.5 Å resolution map of the protein purified from plasma and glycerol molecules, a cryoprotectant, in the case of the recombinant protein[12].

The structures of human plasma holo and presumed apo RBP4 were published more than 20 years ago and revealed a well-defined conformational transition involving a loop at the entrance of the ligand binding site[11]. A similar situation was described for the crystals of bovine RBP4[17]. The crystals used for that study had been prepared by microdialysis using protein purified from human plasma and most surprisingly still diffracted extremely well when recently exposed at the ESRF.

We present here the high resolution three-dimensional crystal structures of human RBP4 naturally lacking bound retinol purified from plasma, urine and amniotic fluid and the 1.5 Å resolution structure of human holo-RBP4 purified from plasma, the highest available for this species. It is remarkable that the data for the holo and "apo" protein purified from plasma could be collected using crystals from the same batch as those of the structures published more than 20 years ago. The significantly increased resolution can be attributed to the amazing developments in the X-ray data collection methods that occurred during the intervening years and was only possible thanks to the stability of protein crystals prepared by equilibrium dialysis. The new improved resolution allowed us to interpret the residual electron density in the cavity of the RBP4 molecule naturally lacking retinol as a fatty acid molecule and not as ordered solvent. We then prepared crystals of RBP4 purified from human urine and amniotic fluid, two sources of protein that contain non fluorescent RBP4 and therefore not bound to retinol and for that reason believed to be the apo form of the protein that has lost its ligand after interacting with the specific receptor. In every case we found density interpretable as a fatty acid in the central cavity of the RBP4 molecule, a result that we confirmed by GC-MS analysis of the samples used in the crystallization experiments. We then tested the ability of the protein to bind fatty acids in vitro by saturating samples with palmitic acid,

known to be present in the natural fluids and lauric acid which is not present and solved the crystal structures of the two complexes.
The interactions RBP4 with palmitic and lauric acid are discussed in detail as well as with all-trans retinol at the significantly improved resolution of 1.5 Å and the conformational changes induced by vitamin deprivation and fatty acid binding.

RESULTS

High resolution structures of human non-fluorescent and holo RBP4 isolated from plasma.

The crystals of plasma non-fluorescent and holo RBP4 used in this study are from the same batch as those of the 2.5 Å resolution study published in 1993. The "apo" protein used to prepare them had been purified using hydrophobic interaction chromatography and the presence of RBP4 was followed using antibodies[18]. Both crystal forms were prepared by equilibrium dialysis using 100 μL cells and kept in their mother liquor in the cold room with the vials that contained the cells sealed with parafilm. When the vials were opened to examine the content of the cells before exposure at the synchrotron, the mother liquor volume was virtually unchanged and the crystals did not look different from those freshly prepared with the same method. Whereas the 2.5 Å resolution model of "apo" RBP4 was refined using 9776 reflections[11] the new data set collected at the synchrotron allowed us to refine with 18786 reflections, 98.3% of those present in the 2.0 Å resolution data set (see Table 1, crystal form 1). In the case of holo RBP4 the 2.5 Å model was refined with 9828 reflections and the current, 1.5 Å resolution model we present here (crystal form 4), with 46,674 reflections. The electron density of both high resolution maps is therefore significantly improved and is clear and continuous for the entire main chain with the exception of two areas where the density is rather poor which are the first 2-3 amino acids and the loop spanning the region of residues 62-67 of both forms. The differences in positions of the side chains of the equivalent models are listed in the supplementary Tables 1 & 2 along with the quality of the density in the high resolution maps. In most cases the improved resolution has led to a better positioning of the side chain while in others, most noticeably the two N terminal amino acids and those in the loop spanning residues 62-67 the ambiguity remains in both the retinol bound and unbound molecule. It is worthwhile mentioning that this loop is also mobile in the other crystal form of holo RBP4 refined at 2.0 Å resolution[10] and that in the H3 crystals it is involved in the intermolecular contacts in the lattice. Supplementary Table 3 lists the differences in positions and B factors in the high resolution models of the side chains that move in non-fluorescent and holo RBP4. As the table shows, the conformational change described in our previous paper on the 2.5 Å structures is confirmed and further supported by the quality of the two high resolution maps. It is worth mentioning that Arg 166 perfectly defined in the maps of non-fluorescent RBP4 becomes disordered in the crystals of the holo protein which can be explained by the role this residue plays in the interaction of the protein with the fatty acid.

Identification of the ligand in the central cavity of RBP4 isolated from human plasma and naturally lacking bound retinol

The 2.5 Å resolution map of non-fluorescent RBP4 showed residual discontinuous electron density in the cavity that is occupied by retinol in the holo protein but the density did not superimpose with the retinol model and was interpreted as probable ordered solvent molecules. The most important conformational change between the models in the presence and absence of retinol involved residues from 34 to 37 and, in particular, the side chains of Leu 35 and Phe 36 were observed to adopt different positions with the second occupying a place close to the alcoholic moiety of retinol in the holo protein. These changes are totally confirmed in the 2.0 Å resolution map but the density in the

cavity becomes continuous and can now be interpreted as a fatty acid molecule. A palmitic acid molecule was fitted to that density in crystal form 1 (Table 1) which shows very clear density starting with the carboxyl group up to C_{11} of the fatty acid, then it becomes weaker. The carboxyl group of the fatty acid interacts with the side chain of Lys 29 with the two oxygens at distances of 3.09 and 3.21 Å from the NZ. It is worth mentioning that in the complex of RBP4 with retinol, Lys 29 does not interact with the ligand but points to the outside of the binding site. The new position that the Lys adopts when the protein is bound to the fatty acid requires the displacement of the side chain of Phe 36 whose position in the protein bound to retinol would generate clashing with both the amino acid side chain and the carboxylate of the fatty acid.
The superficial position of Lys 29, exposed to the solvent when RBP4 is bound to retinol is occupied by the side chain of Arg 166 when the fatty acid is bound instead, the latter is more exposed and partially disordered in the complex of the protein with retinol. The side chains of the two basic amino acids are in contact in the two complexes with that of Asp 31 which is placed in virtually identical positions in the two complexes.

High resolution structures of non-fluorescent human RBP4 isolated from urine and amniotic fluid.

The presence of RBP4 in human urine was detected very early on and it was also observed that the protein concentration in this fluid could be used as a marker of the function of the proximal renal tubule[9]. It was also reported that in patients with glomerular proteinuria more than 80% of the protein molecules lack retinol bound and therefore this biological fluid can be considered as a good source of "apo" RBP4[8]. The non or very weakly fluorescent protein isolated from urine can be readily converted into holo RBP4 by simply saturating with retinol.
Amniotic fluid derives its proteins, at the beginning of gestation from the maternal plasma, but after the kidneys of the foetus begin to function, it becomes increasingly the product of foetal urine and has therefore been assimilated to the latter though it is now clear that it is much more complicated than a waste liquid and contains many key factors of foetal growth[19]. Using samples obtained during weeks 10-33 of gestation, the presence of RBP4 in amniotic fluid was reported, both in the "apo" and holo forms in approximately equal molar quantities[20]. Therefore amniotic fluid is also another source of non or very weakly fluorescent RBP4.
In fully saturated RBP4 the ratio of absorbance at 280 to absorbance at 330 nanometers is about 1 and increases as the samples are progressively depleted from retinol[21].
Our samples of urine and amniotic fluid had ratios A_{280}/A_{330} = 3.6 (urine) and 3.2 (amniotic fluid). Therefore we expected a relatively low percentage of molecules bound to retinol and a majority in the "apo" form. Although the presence of minute amounts of retinol in our samples was confirmed by mass spectrometry we decided not to extract our samples destined to crystallization with organic solvents to avoid introducing the artefact of the presence of solvent molecules in the protein cavity.
Using the hanging drop vapour diffusion method we prepared crystals of RBP4 isolated from both urine and amniotic fluid that are isomorphous to the non-fluorescent crystals of the protein purified from plasma. The data collection and refinement statistics of the models are listed in Table 1 (crystal forms 2 & 3). Notice that the crystals of urine RBP4 diffract to a resolution of 1.5 Å, the highest we have found for this protein. In both cases we observe in the ligand binding site continuous residual electron density that can be easily interpreted as a fatty acid. Figure 1 shows the electron density of the ligand in the crystals prepared with RBP4 isolated from urine. In neither case were we able to identify a partial population of retinol bound RBP4 which can be explained either by the presence of electron density too weak to be interpreted or by the selection of one of the two molecular populations by the process of crystallization. In both cases we fitted a model of palmitic acid to the density present in the interior of the ligand-binding cavity. The addition of a large excess of the ligand did not apparently produce any changes and a comparison of crystal forms 2 & 3 with

5 & 6, i.e. prepared with the protein as purified from the source and alternatively with the sample saturated with palmitic acid did not reveal any significant differences.

Mass spectrometric analysis of the ligands bound to non-fluorescent RBP4 isolated from urine and amniotic fluid.

The identity and occupancy of the major ligands bound in the cavity of non-fluorescent RBP4 isolated from urine and amniotic fluid were investigated using standard gas chromatography tandem mass spectrometry methods applied after lipid methylation and extraction with organic solvents[22]. Figure 2 shows a typical elution profile indicating the relative abundance of the fatty acids bound to RBP4 purified from urine samples as a function of the retention time (RT). The internal standard is heptadecanoic acid (RT=28.03 min), chosen to allow an accurate determination of the predominant fatty acid. The most abundant species is by far palmitic acid but trace amounts of palmitoleic, oleic and stearic acid were also detected. Palmitic acid occupancy was estimated to be about 72 % and stearic acid occupancy about 4-5 % based on a comparison of the areas under the peaks of the ligand extracted from a known amount of the protein and a known amount of the internal standard. Similar results were obtained with the amniotic fluid samples.
The presence of residual retinol bound to non-fluorescent RBP4 was also confirmed by LC-MS/MS analysis of the ligand extracted from urinary and amniotic fluid RBP4. In both cases, we identified the m/z 269 ion, corresponding to the loss of water from the protonated retinol molecule, whose MS/MS spectrum is characteristic of this ligand (Supplementary figure S-1)
We did not attempt to estimate the amount of retinol bound in the non-fluorescent samples that we know is marginal based on the A_{280}/A_{330} ratio.

Ligand binding to RBP4

The common characteristic of the two types of ligand that can bind to RBP4 is that they are both amphipathic with two different polar ends: an alcohol group in one case and a carboxyl group in the other. In both cases the ligands bind with their polar group exposed to the surface of the protein molecule and their hydrophobic tails buried in the beta barrel core. Supplementary Tables S4-S6 list the closest contacts of retinol, palmitate and laurate. Those in contact with both retinol and the fatty acids are only four, Leu 35, Phe 36, Met 88 and Tyr 90 (evidenced in yellow in the tables). The position of the first two plays a crucial role in determining which of the two ligands can fit into the binding cavity. There is also one water molecule conserved in all the structures that we have examined, it is positioned deep inside the hydrophobic cavity and is in contact with polar groups present nearby. Figure 3-a is a stereo view of the α carbon chain trace of the protein with the two ligands represented in different colours. Figure 3-b shows the electron density of the 2 ligands in the maps at 1.5 Å resolution and in the original crystals (Form 1) that allowed us to identify the fatty acid and in Figure 3-c we show the main side chains in contact with the two ligands. The relative position of Leu 35 and Phe 36 in the two complexes explains also the significantly reduced affinity of the carrier protein for TTR when complexed with the fatty acid. Since we now know that circulating non-fluorescent RBP4 is not necessarily the apo protein but is more likely to be fatty acid bound, this selectivity for TTR binding of the two complexes may well have an interesting physiological role.
We have also calculated the solvent accessible volume of the ligand-binding cavity of the molecules present in the eight crystal forms that we have studied with the program CASTp[46]. The results of these calculations are listed in supplementary Table 7 and show consistently a very small variability in the volume of the cavity that accommodates the fatty acids and a significantly larger volume when the ligand is retinol.

It is well known that RBP4 can bind different retinoids but our conclusion after examination of the data we present here is that it is not surprising that it can also bind fatty acids.

DISCUSSION

Plasma retinol-binding protein, RBP4, has so far been always considered to be highly specific for retinoids and, in particular, for one ligand, i.e. all-trans retinol. In fact, its secretion by the liver is only triggered by the presence of all-trans retinol bound to the protein and in vitamin A deficiency, RBP4 accumulates in the hepatocytes and is only released after retinol repletion[1,23].

In addition to its role as a selective transporter of retinol, a second function was assigned to RBP4, i.e. that of an adipokine[24], a cell-to-cell signaling molecule that influences energy metabolism and behaves like a marker of insulin sensitivity and adiposity. An increased level in plasma RBP4 is observed in type 2 diabetes mellitus, impaired glucose tolerance, obesity and cardiovascular disease[25].

It has been known for a long time that RBP4 is also synthesized extra-hepatically, mainly in the adipocytes that have the second highest expression level of the protein, about 20-40% of the amount synthesized by the liver[26]. Therefore, the observation that the protein of extra-hepatic origin plays no role in retinoid metabolism poses a question that has not yet received an answer: what is the physiological role of extra-hepatic RBP4?[27]. A reasonable proposal is that it should have a function related to its tissue of origin and our observation that RBP4 can circulate bound to a fatty acid opens up new possibilities to explain this possible dual role. The first, and better known function of RBP4, is in retinoid metabolism while the second, is as a transporter of fatty acids in plasma and is most probably related to its function as an adipokine and its alterations in adipocyte lipid metabolism[28]. Recently, adipocyte fatty acid-binding protein, also known as FABP4, has been suggested as a third adipokine produced by adipocytes, in addition to leptin and adiponectin[29]. Similarly, RBP4 was known first to be an adipokine and is now shown to be a fatty acid-binding protein which suggests similar roles for both RBP4 and FBP4 that present also some degree of structural similarity[30].

Our observation that RBP4, isolated from urine and amniotic fluid and believed to be apo, because not bound to the fluorescent all-trans retinol is, in fact, liganded to a fatty acid molecule raises the question of what are the concentrations of the two forms of the protein present in normal and pathological fluids. An evaluation of the two populations in health and metabolic disease may provide new clues as to the exact role of this protein in lipid metabolism.

The different affinity of RBP4 when saturated with retinol or with a fatty acid for TTR is probably the cause of the presence of mostly the second species in human urine and amniotic fluid. However, we have also detected traces of retinol in urine and amniotic fluid samples probed with conventional mass spectrometry. It is possible that the protein isolated from those fluids may be the result of an interaction of holo RBP4 saturated with retinol and the specific receptor STRA6 but equally probable is the non-hepatic origin of the protein saturated with the fatty acid.

To summarize our results we can state that from now on we should not consider RBP4 any more as a specific transporter of retinol but rather as a lipid binding protein with a specificity that has yet to be evaluated as are the binding constants of all its possible ligands. The conformational changes that we have described that explain the different affinity of the two complexes with the ligands for TTR are minimal but they can still explain the different destiny of the two forms of RBP4. Yet the complex RBP4-fatty acids ends up in urine only in the presence of a glomerulopathy and not in normal individuals and so its affinity for TTR or eventually for other not yet identified plasma components should be explored. The most important unanswered question is the fate of the protein that has interacted with the STRA6 receptor which is not likely to be the species that we believed was apo RBP4 though we cannot exclude the possibility that in the process of retinol release the protein may take up a fatty acid molecule to fill up the empty hydrophobic ligand-binding site. The

second function of RBP4 as a fatty acid transporter and its role in lipid metabolism are new areas that definitely deserve to be explored in depth.

METHODS

Methods and any associated references are available in the online version of the paper.

Accession codes, PDB: The atomic coordinates and structure factors of all the crystal forms in Table 1 have been deposited in the Protein Data Bank, the accession codes are given in the table.

References

1. Goodman, D.S. (1984). Plasma retinol-binding protein. In "The Retinoids" (M.B. Sporn, A.B. Roberts & D.S. Goodman, Eds.) vol 2, pp41-88. Academic Press, New York
2. Schiefner, A. & Skerra, A. The menagerie of human lipocalins: a natural protein scaffold for molecular recognition of physiological compounds. *Acc. Chem. Res.* **48**, 976-985 (2015).
3. Raz, A. & Goodman, D.S. The interaction of thyroxine with human plasma prealbumin and with the prealbumin-retinol-binding protein complex. *J. Biol. Chem.* **244**, 3230-3237 (1969).
4. van Jaarsveld, P.P., Edelhoch, H., Goodman, D.S. & Robbins, J. The interaction of human plasma retinol-binding protein and prealbumin. *J. Biol. Chem.* **248**, 4698-4705 (1973).
5. Richardson, S.J. & Cody, V. (editors) Recent advances in Transthyretin evolution, structure and biological functions, Springer Verlag (2009).
6. Kawaguchi, R., Zhong, M., Kassai, M., Ter-Stepanian, M. & Sun, H. Vitamin A transport mechanism of the multitransmembrane cell-surface receptor STRA6. *Membranes (Basel).* **5**, 425-453 (2015) .
7. van Bennekum, A.M., Wei, S., Gamble, M.V., Vogel, S., Piantedosi, R., Gottesman, M., Episkopou, V. & Blaner, W.S. Biochemical basis for depressed serum retinol levels in transthyretin-deficient mice. *J. Biol. Chem.* **276**, 1107-1113 (2001).
8. Fex, G. & Hansson, B. Retinol-binding protein from human urine and its interaction with retinol and prealbumin. *Eur. J. Biochem.* **94,** 307-313 (1979).
9. Norden, A.G., Lapsley, M. & Unwin, R.J. Urine retinol-binding protein 4: a functional biomarker of the proximal renal tubule. *Adv. Clin. Chem.* **63**, 85-122 (2014).
10. Cowan, S.W., Newcomer, M.E. & Jones, T.A. Crystallographic refinement of human serum retinol binding protein at 2 Å resolution. *Proteins.* **8**, 44-61 (1990).
11. Zanotti, G., Ottonello, S., Berni, R. & Monaco, H.L. Crystal structure of the trigonal form of human plasma retinol-binding protein at 2.5 Å resolution. *J. Mol. Biol.* **230**, 613-624 (1993).
12. Greene, L.H., Chrysina, E.D., Irons, L.I., Papageorgiou, A.C., Acharya, K.R. & Brew, K. Role of conserved residues in structure and stability: tryptophans of human serum retinol-binding protein, a model for the lipocalin superfamily. *Protein Sci.* **10**, 2301-2316 (2001).
13. Chen, Y., Clarke, O.B., Kim, J., Stowe, S., Kim, Y.K., Assur, Z., Cavalier, M., Godoy-Ruiz, R., von Alpen, D.C., Manzini, C., Blaner, W.S., Frank, J., Quadro, L., Weber, D.J., Shapiro, L., Hendrickson, W.A. & Mancia, F. Structure of the STRA6 receptor for retinol uptake. *Science.* **353,** aad8266 (2016). doi: 10.1126/science.aad8266.
14. Bychkova, V.E., Dujsekina, A.E., Fantuzzi, A., Ptitsyn, O.B. & Rossi, G.L. Release of retinol and denaturation of its plasma carrier, retinol-binding protein. *Fold Des.* **3**, 285-291 (1998) .
15. Monaco, H.L., Rizzi, M. & Coda, A. Structure of a complex of two plasma proteins: transthyretin and retinol-binding protein. *Science.* **268**, 1039-1041 (1995).

16. Monaco, H.L. The transthyretin-retinol-binding protein complex. *Biochim. Biophys. Acta*. **1482**, 65-72 (2000).
17. Zanotti, G., Berni, R. & Monaco, H.L. Crystal structure of liganded and unliganded forms of bovine plasma retinol-binding protein. *J. Biol. Chem*. **268**, 10728-10738 (1993).
18. Monaco, H.L., Zanotti, G., Ottonello, S. & Berni, R. Crystallization of human plasma apo-retinol-binding protein. *J. Mol. Biol.* **178**, 477-479 (1984).
19. Underwood, M.A., Gilbert, W.M. & Sherman, M.P. Amniotic fluid: not just fetal urine anymore. *Journal of Perinatology* **25,** 341–348 (2005).
20. Wallingford, J.C., Milunsky, A. & Underwood, B.A. Vitamin A and retinol-binding protein in amniotic fluid. *Am. J. Clin. Nutr.* **38**, 377-381 (1983).
21. Heller, J. & Horwitz, J. Conformational changes following interaction between retinol isomers and human retinol-binding protein and between the retinol-binding protein and prealbumin. *J. Biol. Chem*. **248**, 6308-6316 (1973).
22. Murphy, R.C. & Axelsen, P.H. Mass spectrometric analysis of long-chain lipids. *Mass Spectrom. Rev.* **30**, 579-599 (2011).
23. Ronne, H., Ocklind, C., Wiman, K., Rask, L., Obrink, B. & Peterson, P.A. Ligand-dependent regulation of intracellular protein transport: effect of vitamin a on the secretion of the retinol-binding protein. *J. Cell Biol.* **96**, 907-910 (1983).
24. Yang, Q., Graham, T.E., Mody, N., Preitner, F., Peroni, O.D., Zabolotny, J.M., Kotani, K., Quadro, L. & Kahn, B.B. Serum retinol binding protein 4 contributes to insulin resistance in obesity and type 2 diabetes. *Nature.* **436**, 356-362 (2005).
25. Christou, G.A., Tselepis, A.D. & Kiortsis, D.N. The metabolic role of retinol binding protein 4: an update. *Horm. Metab. Res.* **44**, 6-14 (2012).
26. Tsutsumi, C., Okuno, M., Tannous, L., Piantedosi, R., Allan, M., Goodman, D.S. & Blaner, W.S. Retinoids and retinoid-binding protein expression in rat adipocytes. *J. Biol. Chem.* **267**, 1805-1810 (1992).
27. Quadro, L., Blaner, W.S., Hamberger, L., Novikoff, P.M., Vogel, S., Piantedosi, R., Gottesman, M.E. & Colantuoni, V. The role of extrahepatic retinol binding protein in the mobilization of retinoid stores. *J. Lipid Res.* 45, 1975-1982 (2004) .
28. von Eynatten, M., Humpert, P.M.. Retinol-binding protein-4 in experimental and clinical metabolic disease. *Expert Rev. Mol. Diagn.* **8**, 289-299 (2008).
29. Kralisch, S. & Fasshauer, M. Adipocyte fatty acid binding protein: a novel adipokine involved in the pathogenesis of metabolic and vascular disease? *Diabetologia.* **56**, 10-21 (2013).
30. Flower, D.R., North, A.C. & Sansom, C.E. The lipocalin protein family: structural and sequence overview. *Biochim. Biophys. Acta*. **1482,** 9-24 (2000).

Acknowledgments
We thank the staff of the ESRF in Grenoble (Proposals MX 1750 & 1841) for assistance during data collection.

Author contributions
M.P. prepared the urine and amniotic fluid protein crystals and solved all the X-ray structures, S.N., & B.M. performed the mass spectrometry experiments. M.G. prepared the urine and amniotic fluid protein samples and interpreted the mass spectrometry results. HLM prepared the old crystals, directed the research and wrote the paper.

Competing financial interests
The authors declare no competing financial interests.

Additional information

Supplementary information is available in the **online version of the paper**. Reprints and permissions information is available online at **http://www.nature.com/reprint/index.html.** Correspondence and requests for materials should be addressed to H.L.M.

Online Methods

Protein Purification.

The preparation of holo[31] and non-fluorescent plasma RBP4 has been described[32]. Briefly, the retinol unliganded RBP4 was purified directly from normal serum using a method that involved three chromatographic steps on: (1) phenyl-Sepharose equilibrated with 1.6 M ammonium sulfate, 0.05 M sodium citrate (pH 6.0) and eluted with a discontinuous pH and ammonium sulfate gradient from the starting buffer to 0.08 M ammonium sulfate, 0.05 M phosphate (pH 7.0); (2) cibacron Blue F3-G-Sepharose equilibrated and eluted with 0.05 M Tris-HCl (pH7.2); (3) Sephadex Gl00 equilibrated and eluted with the same buffer. RBP4 was detected using commercially available polyclonal antibodies. The product of this purification method was electrophoretically homogeneous, more than 98 % free of retinol as judged by its absorption and fluorescence spectra, and fully active with respect to its capacity to bind retinol.
Human RBP4 was also isolated from the urine of hemodialized patients (1.5 L) and from human amniotic fluid (2 L) obtained by pooling discarded amniocentesis samples collected in the weeks 16-18 of pregnancy. The fluids were saturated to 80% with ammonium sulfate and the precipitated proteins, after centrifugation at 10 000 g for 1 h, were suspended in 50 mM Tris-HCl, 0.02% NaN_3, 5 mM EDTA, 150 mM NaCl, pH 8.0, dialyzed against the same buffer and fractioned by gel filtration on a 4x100 cm Sephadex G100 column at 4 °C. Proteins eluting after the albumin peak were pooled, equilibrated in 6.25 mM Bis-Tris-propane, pH 7.5 and separated on a 2.6x30 cm high performance Q-Sepharose column equilibrated with the same buffer (buffer A) and connected to an Äkta prime liquid chromatography system (GE Healthcare Life Sciences). The elution was performed with a 375 min linear gradient from 0-100% of 6.25 mM Bis-Tris-propane, pH 9.5, 350 mM NaCl, (buffer B) and monitored at 280 nm. The Retinol binding protein containing fractions were pooled, concentrated and submitted to gel filtration on a Superdex G75 column (GE Healthcare Life Sciences) equilibrated and eluted with 20 mM Tris-HCl buffer, pH 8.0, 150 mM NaCl. The homogeneity of the protein was checked by SDS-PAGE analysis in 17% gels and by N-terminal sequence determination in a Hewlett-Packard model G 1000 A sequencer (Centro Grandi Strumenti, University of Pavia).
The protein concentration was determined from the specific extinction coefficient at 280 nm, using an $\varepsilon = 1.7$ mL mg^{-1} cm^{-1}. The ratio A_{280}/A_{330} was 3.6 for the protein purified from urine and 3.2 for that purified from amniotic fluid.

Crystallization.

The preparation of the old holo and plasma retinol deprived RBP4 crystals by equilibrium dialysis has been described[11]. The new crystallization experiments were performed for all the samples with the hanging drop vapour diffusion method using the established conditions[33]. Each drop was prepared mixing 1 μL of a 20 mg/mL protein solution (in 20 mM Tris-HCl buffer, pH 8.0, 150 mM NaCl) with the same volume of precipitant solution (100 mM Hepes, pH 7.5, 4.3 M NaCl) and equilibrated versus a volume of 0.35 mL in the reservoir. The crystallization experiments were kept

at 20°C and periodically checked. Large rhombohedral shaped crystals were obtained sometimes after only one or two days.
Samples of RBP4 purified from both urinary and amniotic fluid were saturated with palmitic acid to prepare co-crystals. To dilute protein solutions (0.5 mg/mL in 20 mM Tris-HCl pH 7.4) 10 times the molar concentration of the fatty acid were added and kept under stirring overnight at 4°C previous to concentration and crystallization. The co-crystals of RBP4 with palmitic acid using both urinary and amniotic fluid protein were prepared using the same conditions as the naturally depleted samples.

2.3. Data collection and processing.

The data used for refinement of all the crystal structures were collected on two beamlines at the European Synchrotron Radiation Facility (ESRF) in Grenoble. The diffraction data were collected from crystals cooled to 100 K after brief immersion into a mixture of 80% mother liquor and 20% glycerol. The data were indexed, integrated and reduced using the programs MOSFLM[34] and Scala[35]. The processed data were converted to structure factors using the program TRUNCATE from the CCP4 suite[36].
A summary of the data collection statistics is given in Table 1.

2.4. Structure determination and refinement.

The high resolution structure of holo-RBP4 was solved using the molecular replacement method as implemented in the program Molrep[37]. The search probe used was the available model to 2.5 Å resolution without retinol and solvent molecules (PDB code 1BRP).
After rigid body refinement of the solution, the model was first refined by simulated annealing, using the program Phenix.refine[38,39], present in the suite Phenix[40]. The next step was a series of several rounds of positional refinement alternated with manual model revisions using the program COOT[41] and the refinement programs Refmac[42] and Phenix.refine. During the process of refinement and model building the quality of the models was controlled using the program PROCHECK[43]. Residual electron density for retinol bound to RBP4 was located and modeled in 2Fo – Fc and Fo – Fc maps obtained from the holoprotein data refined against the apoprotein model refined at high resolution.
The models were finally subjected to final rounds of TLS refinement. Solvent molecules were added to the models in the final stages of refinement according to hydrogen-bond criteria and only if their *B* factors refined to reasonable values and if they improved the *R* free.
The diffraction data and refinement statistics of the models are summarized in Table 1.

2.5. Mass spectrometry

2.5.1 Mass spectrometric identification of fatty acids bound to non-fluorescent RBP4 isolated from urine and amniotic fluid.

Fatty acid identification was performed essentially as previously described[44]. Briefly, the RBP-bound fatty acids were methylated by dissolving and sonicating a known amount of the desalted and liophylized protein (typically 2-3 mg) in 5 mL methanol-acetyl chloride (50:1, v/v). An internal standard (heptadecanoic acid, 99% pure, Sigma) was added before incubation at 70°C for 4 hrs under magnetic stirring. After cooling to room temperature, 3 mL of 0.6% K_2CO_3 and 500 µL of hexane were added. Vials were shaken for 60 s and centrifuged for 5 min at 4000 rpm. 100 µL of FAME-containing upper phase were transferred to autosampler vials and analyzed by GC-MS.

Analyses were carried out with a Thermo Scientific DSQII single quadrupole GC-MS system (Xcalibur MS Software Version 2.1), equipped with a Restek Rtx-5MS (30 m x 0.25 mm ID x 0.25 µm film thickness) capillary column, with helium as carrier gas at 1 mL/min constant flow. Sample injections of 1 µL were performed in split mode (split flow 10 mL/min, split ratio 1:10) and the injector temperature was 250°C. The oven temperature was held at 45°C for 4 min, increased to 175°C by a temperature ramp of 13°C/min and held for 27 min, then ramped at 4°C /min to 215°C and held for 35 min. The MS transfer line temperature was 250°C and the ion source temperature 250°C. Mass spectral analyses were carried out in full scan mode, over the mass range of 35-650 amu. Quantitative results were obtained by comparing the peak area of FAME analytes to that of the internal standard.

2.5.2 Mass spectrometric detection of retinol bound to non-fluorescent RBP4 isolated from urine and amniotic fluid.

The extraction of residual retinol bound to amniotic and urinary RBP4 was performed adding to 2mL of 2 mg/mL protein solution 3 mL of $CHCl_3/CH_3OH$ 2:1 v/v. The samples were centrifuged at 3600 rpm for 10 min, the lower lipid-rich layer was collected and evaporated to dryness. Samples were reconstituted in 500 µL of ACN/IPA/H_2O (65:30:5 v/v/v) before LC-MS/MS analysis and 100 µL of sample were injected into the LC-MS/MS system.
The system used for LC-MS analyses was a Surveyor LC coupled with an ion-trap mass spectrometer LCQ (Thermo Scientific, San Jose, CA) equipped with an electrospray ionization (ESI) source and controlled by Xcalibur software 2.0.7 (Thermo Scientific). Experiments were carried out in positive ion mode under constant instrumental conditions: source voltage 5.0 kV, capillary voltage 46 V, capillary temperature 210 °C, tube lens voltage 55 V. Mass spectra were acquired in the mass range of 200-2000 *m/z* by scanning the magnetic field in 200 ms. The system was run in automated LC−MS/MS mode and using a Surveyor HPLC system (Thermo Finnigan) equipped with a Jupiter 4u Proteo column (Phenomenex, Torrance, CA), 4 µm, 150 × 2.0 mm. The elution was performed using 0.1% HCOOH in distilled water (solvent A) and 0.1% HCOOH in acetonitrile (solvent B), with a flow rate of 0.2 mL/min; elution started with 98% solvent A for 5 min followed by a linear gradient from 98 to 0% A in 40 min, 0% A for 5 min, and 98% A for 10 min. MS/MS spectra obtained by collision-induced dissociation were performed with an isolation width of 2 Th (m/z), and the activation amplitude was around 35% of the ejection-radiofrequency amplitude of the instrument.

2.6. Analysis of the models.

The superposition of the models matching the secondary structure was performed using the subroutine SSM Superposition of the program Coot[45]. The distances between the ligand and protein atoms were calculated with the CCP4 program CONTACT (Tadeusz Skarzynski, Imperial College, London, 1.12.88). Figures of the structures were prepared and rendered with PyMOL (http://www.pymol.org).

References

31. Ottonello, S., Maraini, G., Mammi M., Monaco, H.L., Spadon, P. & Zanotti, G. Crystallization and preliminary X-ray data of human plasma retinol-binding protein. *J. Mol. Biol*. **163**, 679-681 (1983).
32. Berni, R., Ottonello, S. & Monaco, H.L. Purification of human plasma retinol-binding protein by hydrophobic interaction chromatography. *Anal. Biochem.* **150,** 273-277 (1985).
33. Monaco, H.L., Zanotti, G., Ottonello, S. & Berni, R. Crystallization of human plasma apo-retinol-binding protein. *J. Mol. Biol.* **178**, 477-479 (1984).
34. Leslie, A.G.W. & Powell, H.R. Processing diffraction data with Mosflm. Evolving methods for macromolecular crystallography. **245**, 41–51 (2007).
35. Evans, P.R. Scaling and assessment of data quality. *Acta Cryst.* **D62**, 72–82 (2006).
36. Winn, M.D., Ballard, C.C., Cowtan, K.D., Dodson, E.J., Emsley, P., Evans, P.R., Keegan, R.M., Krissinel, E.B., Leslie, A.G., McCoy, A., McNicholas, S.J., Murshudov, G.N., Pannu, N.S., Potterton, E.A., Powell, H.R., Read, R.J., Vagin, A. & Wilson, K.S. Overview of the CCP4 suite and current developments. *Acta Crystallogr. D Biol. Crystallogr.* **67**, 235-242 (2011).
37.Vagin, A. & Teplyakov, A. An approach to multi-copy search in molecular replacement. *Acta Crystallogr. D Biol. Crystallogr*. **56**, 1622–1624 (2000).
38. Afonine, P.V., Grosse-Kunstleve, R.W., Adams, P.D. A robust bulk-solvent correction and anisotropic scaling procedure**.** *Acta Crystallogr. D Biol. Crystallogr.* **61**, 850-855 (2005).
39. Afonine, P.V., Grosse-Kunstleve, R.W., Echols, N., Headd, J.J., Moriarty, N.W., Mustyakimov, M., Terwilliger, T.C., Urzhumtsev, A., Zwart, P.H. & Adams, P.D. Towards automated crystallographic structure refinement with phenix.refine. *Acta Crystallogr. D Biol. Crystallogr.* **68**, 352-67 (2012).
40. Adams, P.D., Afonine, P.V., Bunkóczi, G., Chen, V.B., Davis, I.W., Echols, N., Headd, J.J., Hung, L.W., Kapral, G.J., Grosse-Kunstleve, R.W., McCoy, A.J., Moriarty, N.W., Oeffner, R., Read, R.J., Richardson, D.C., Richardson, J.S., Terwilliger, T.C. & Zwart, P.H. PHENIX: a comprehensive Python-based system for macromolecular structure solution. *Acta Crystallogr. D Biol. Crystallogr*. **66,** 213-221 (2010).
41. Emsley, P., Lohkamp, B., Scott, W.G. & Cowtan, K. Features and development of Coot. *Acta Crystallogr. D Biol. Crystallogr.* **66,** 486-501 (2010).
42.Murshudov, G.N., Vagin, A.A. & Dodson, E.J. Refinement of macromolecular structures by the maximum-likelihood method. *Acta Crystallogr. D Biol. Crystallogr*. **53**, 240–255 (1997).
43. Laskowski, R.A., MacArthur, M.W., Moss, D.S. & Thornton, J.M. PROCHECK: A program to check the stereochemical quality of protein structures. *J. Appl. Crystallogr*. **26**, 283–291 (1993).
44.Kragh-Hansen, U., Campagnoli, M., Dodig, S., Nielsen, H., Benko, B., Raos, M., Cesati, R., Sala, A., Galliano, M. & Minchiotti, L. Structural analysis and fatty acid-binding properties of two Croatian variants of human serum albumin. *Clin. Chim. Acta*. **349**, 105-112 (2004).
45. Krissinel, E. & Henrick, K. Secondary-structure matching (SSM), a new tool for fast protein structure alignment in three dimensions. *Acta Crystallogr. D Biol. Crystallogr*. **60**, 2256-68 (2004).
46. Dundas, J., Ouyang, Z., Tseng, J., Binkowski, A., Turpaz, Y. & Liang, J. CASTp: computed atlas of surface topography of proteins with structural and topographical mapping of functionally annotated residues. *Nucleic Acids Res.* **34** (Web Server issue):W116-W118 (2006).

Table 1 Data collection and refinement statistics.

RBP4 Data set	Non-fluorescent human RBP4 (plasma)	Non-fluorescent human RBP4 (urine)	Non-fluorescent human RBP4 (amniotic fluid)	Holo human plasma RBP4	Human RBP4 saturated with palmitate (urine)	Human RBP4 saturated with palmitate (amniotic fluid)	Human RBP4 saturated with laurate (urine)	Human RBP4 saturated with laurate (amniotic fluid)
Space group	H3	H3	H3	H3	H3	H3	H3	H3
Crystal form	1	2	3	4	5	6	7	8
a (Å)	103.77	102.68	102.58	103.10	102.79	102.84	102.82	102.61
b (Å)	103.77	102.68	102.58	103.10	102.79	102.84	102.82	102.61
c (Å)	73.94	73.18	73.28	73.55	73.63	73.16	73.27	73.13
α	90	90.0	90.0	90	90.0	90.0	90.0	90.0
β	90	90.0	90.0	90	90.0	90.0	90.0	90.0
γ	120	120.0	120.0	120	120.0	120.0	120.0	120.0
Molecules in the asymmetric unit	1	1	1	1	1	1	1	1
Resolution range (Å)	40.0 – 2.0	56.49 – 1.50	56.53 - 1.68	38.16 - 1.50	56.74 - 1.59	56.53 - 1.50	56.58 - 1.60	56.47 - 1.60
Observed reflections	86,301	105,972	77,722	201,042	88,650	92,745	170,333	172,447
Independent reflections	19,780	44,537	31,219	46,674	35,401	43,348	37,778	37,622
Multiplicity	4.4 (4.2)	2.4 (2.3)	2.5 (2.4)	4.3 (4.3)	2.5 (2.5)	2.1 (2.1)	4.5 (4.2)	4.6 (4.2)
Rmerge (%)	10.6 (49.1)	3.7 (44.3)	6.7 (45.0)	5.8 (46.2)	5.3 (46.6)	4.2 (36.6)	4.8 (44.4)	5.4 (48.1)
$\langle I/\sigma(I)\rangle$	7.9 (2.5)	10.5 (1.8)	7.8 (2.0)	12.6 (2.8)	9.2 (2.0)	9.7 (1.9)	13.2 (2.6)	12.8 (2.6)
Completeness (%)	98.5 (98.3)	96.7 (96.3)	95.3 (93.7)	99.5 (99.4)	90.9 (92.3)	93.8 (94.4)	99.1 (98.5)	99.3 (98.7)
Reflections in refinement	18,786	43,086	29,609	44,136	33,661	41,174	35,785	35,652
Rcryst (%)	17.20	15.65	16.95	17.97	17.00	16.97	16.99	17.36
Rfree (%) (test set 5%)	23.03	18.36	19.71	20.96	21.17	19.53	19.67	20.50
Protein atoms	1,408	1,416	1,408	1,408	1,416	1,416	1,416	1,416
Ligand atoms	19	20	20	22	20	20	16	16
Water molecules	78	124	89	77	113	102	110	109
r.m.s.d. on bond lengths (Å)	0.003	0.004	0.003	0.003	0.003	0.004	0.003	0.003
r.m.s.d. on bond angles (Å)	0.651	0.702	0.684	0.641	0.663	0.767	0.618	0.678
Planar groups (Å)	0.002	0.003	0.002	0.004	0.002	0.003	0.002	0.003
Chiral volume dev. ($Å^3$)	0.032	0.041	0.037	0.040	0.038	0.043	0.040	0.042
Average B factor ($Å^2$)	34.17	30.39	36.23	28.20	33.61	27.38	27.19	27.22
Protein atoms	34.37	30.37	36.29	28.41	33.72	27.27	27.25	27.18
Ligand atoms	40.63	37.88	41.98	27.13	35.89	34.68	38.25	40.74
Solvent atoms	29.11	29.35	33.90	24.61	31.80	27.39	24.77	25.78
ESRF beamline Date of data collection	ID29 07/16/2015	ID23-1 11/27/2015	ID29 02/18/2016	ID29 03/14/2015	ID29 02/18/2016	ID29 02/18/2016	ID29 02/18/2016	ID29 02/18/2016
PDB accession code	5NTY	5NU2	5NU6	5NU7	5NU8	5NU9	5NUA	5NUB

* The values in parentheses refer to the highest resolution shells.

[a] Rmerge = $\Sigma h \Sigma i \mid Ih - \langle Ih \rangle / \Sigma h \Sigma i \langle Ih \rangle$ where $\langle Ih \rangle$ is the mean intensity of the *i* observations of reflection *h*.

[b] Rcryst = $\Sigma \mid |Fobs| - |Fcalc| \mid / \Sigma |Fobs|$, where |Fobs| and |Fcalc| are the observed and calculated structure factor amplitudes, respectively. Summation includes all reflections used in the refinement.

[c] Rfree = $\Sigma \mid |Fobs| - |Fcalc| \mid / \Sigma |Fobs|$, evaluated for a randomly chosen subset of 5% of the diffraction data not included in the refinement.

[d] Root mean square deviation from ideal values.

Figure captions

Figure 1 - Residual electron density in the binding site of the crystals prepared with non-fluorescent RBP4 isolated from human urine.

The stereo view is of a 2Fobs – Fc map contoured at a 1.0 σ level. A model of palmitic acid, the most abundant fatty acid bound to the protein according to our mass spectrometry results is represented along with the electron density present in the ligand-binding site. Similar results were observed for crystal forms 1 (plasma) and 3 (amniotic fluid) but crystal form 2 (see Table 1) was chosen because of the higher resolution data (1.5 Å) available.

Figure 2 - Mass spectrometric identification of fatty acids bound to non-fluorescent RBP4 isolated from urine and amniotic fluid.

The gas chromatography elution profile shows the peaks corresponding to the different fatty acids converted into their more volatile methyl ester derivatives as a function of their retention times. The sample was purified from urine and the internal standard was heptadecanoic acid. The palmitic acid occupancy was estimated to be 72 % based on a comparison of its peak area and that of the internal standard. Similar results were obtained with samples purified from amniotic fluid.

Figure 3 - Ligand binding to human RBP4

A – Stereo view of the α carbon chain trace of the protein with the models of retinol (green) and palmitate (red) superimposed. The models of the plasma protein complexes were superimposed using the program LSQKAB.
B – Ribbon representation of RBP4 with the Fobs-Fc electron density of retinol (crystal form 4) and palmitate in the plasma non-fluorescent crystals (crystal form 1, P in the figure) and in the highest resolution complex, purified from amniotic fluid and saturated with palmitate (crystal form 7, AF in the figure). The electron density of the Fobs-Fc maps was contoured at a 1.5 σ level.
C – Main amino acid side chains in contact with retinol (left) and palmitate (right) in the ligand binding cavity. The residues in contact with the two ligands are coloured orange. Notice the position of the conserved water molecule 201 and the contacts of the alcohol and carboxylate atoms with the protein. The latter is also in contact with water molecule number 264.
D – The role of Phe 36 in the binding of the two ligands. Its position is shown in green when retinol occupies the ligand binding cavity and in red when palmitate is bound instead. The relative position of this side chain is crucial in discriminating which of the ligands is present in the cavity.

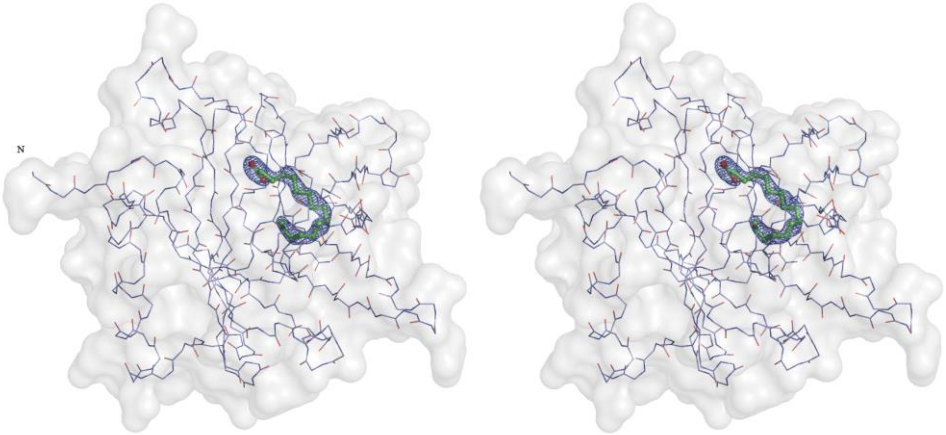

Figure 1

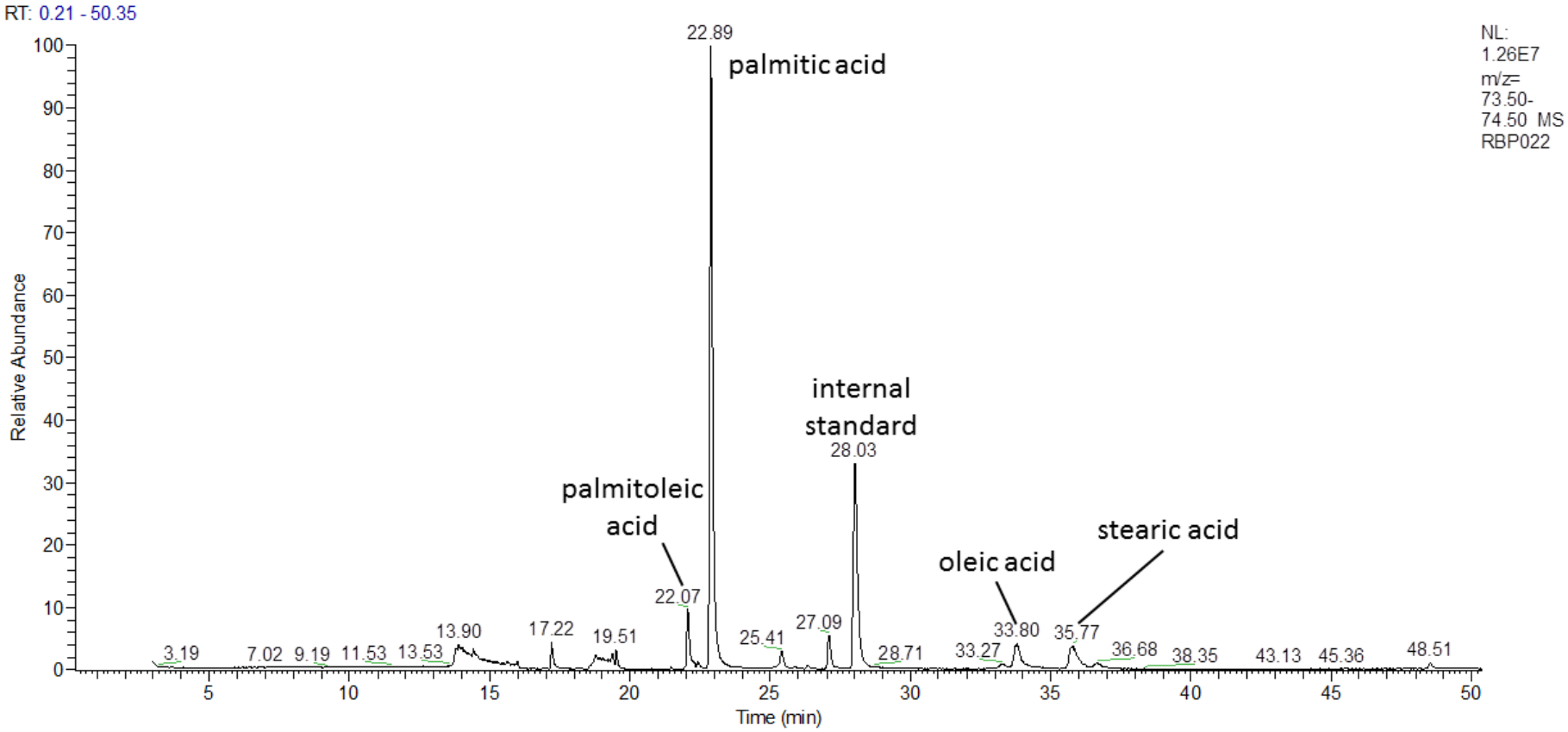
RT: 0.21 - 50.35
NL:
1.26E7
m/z=
73.50-
74.50 MS
RBP022
Relative Abundance
Time (min)
22.89
palmitic acid
internal
standard
28.03
palmitoleic
acid
22.07
oleic acid
33.80
stearic acid
35.77
3.19
7.02
9.19
11.53
13.53
13.90
17.22
19.51
25.41
27.09
28.71
33.27
36.68
38.35
43.13
45.36
48.51

Figure 2

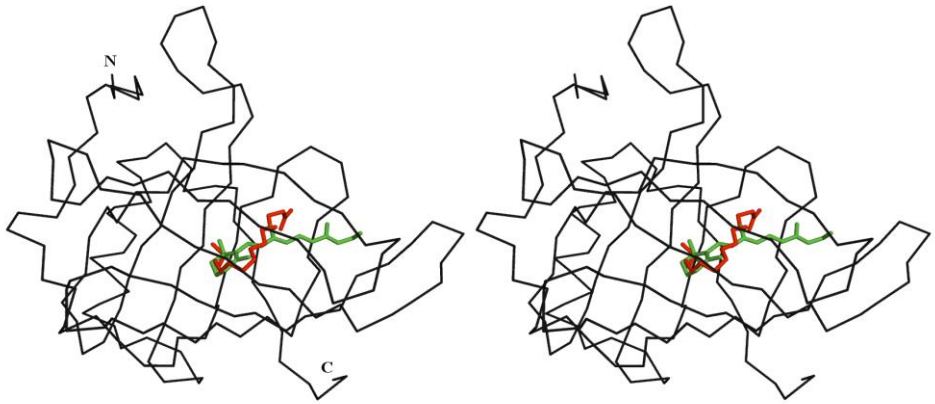

Figure 3 (A)

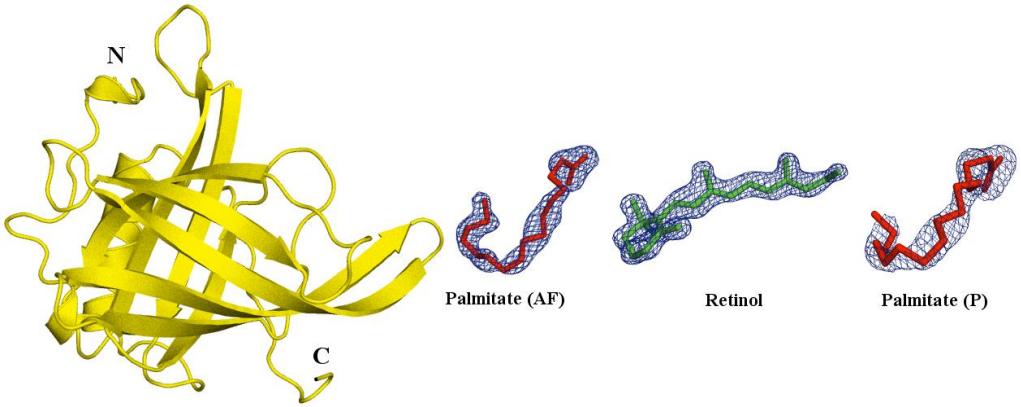

Figure 3 (B)

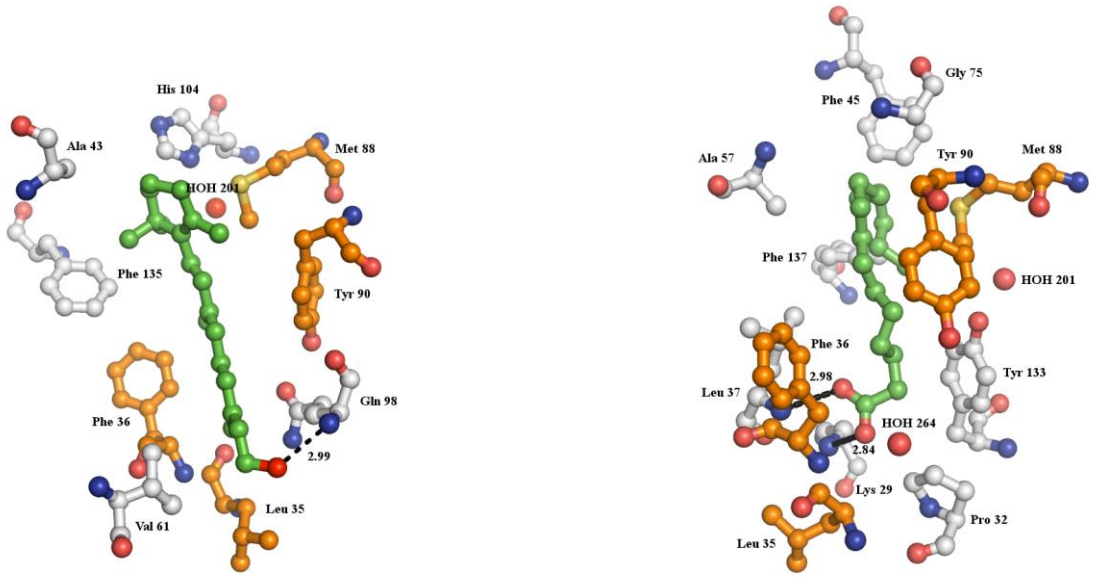
His 104
Ala 43
Met 88
HOH 201
Phe 135
Tyr 90
Gln 98
Phe 36
2.99
Leu 35
Val 61
Gly 75
Phe 45
Ala 57
Tyr 90
Met 88
Phe 137
HOH 201
Phe 36
Tyr 133
Leu 37
2.98
HOH 264
2.84
Lys 29
Pro 32
Leu 35

Figure 3 (C)

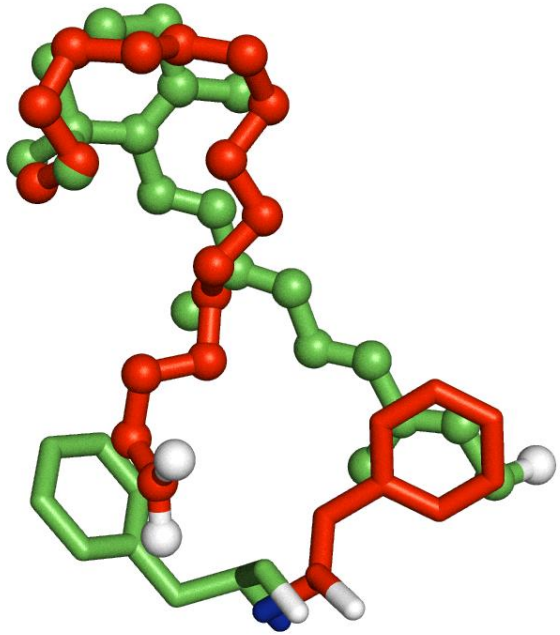

Figure 3 (D)